# Bioassociation of U(VI) and Eu(III) by plant (Brassica napus) suspension cell cultures – A spectroscopic investigation

Jessat, J.; Sachs, S.; Moll, H.; John, W.; Steudtner, R.; Hübner, R.; Bok, F.; Stumpf, T.;

Originally published:

April 2021

**Environmental Science and Technology 55(2021)10, 6718-6728**

DOI: https://doi.org/10.1021/acs.est.0c05881

# Bioassociation of U(VI) and Eu(III) by plant (*Brassica napus*) suspension cell cultures – A spectroscopic investigation

Jenny Jessat[1], Susanne Sachs[1]*, Henry Moll[1], Warren John[1], Robin Steudtner[1], René Hübner[2], Frank Bok[1], and Thorsten Stumpf[1].

[1] Helmholtz-Zentrum Dresden-Rossendorf, Institute of Resource Ecology, Bautzner Landstraße 400, 01328 Dresden, Germany.

[2] Helmholtz-Zentrum Dresden-Rossendorf, Institute of Ion Beam Physics and Materials Research, Bautzner Landstraße 400, 01328 Dresden, Germany.

ABSTRACT: In this study, we investigated the interaction of U(VI) and Eu(III) with *Brassica napus* suspension plant cells as a model system. Concentration-dependent (0-200 µM) bioassociation experiments showed that more than 75% of U(VI) and Eu(III) were immobilized by the cells. In addition to this phenomenon, time-dependent studies for 1 to 72 h of exposure showed a multi-stage bioassociation process for cells that were exposed to 200 µM U(VI), where, after initial immobilization of U(VI) within 1 h of exposure, it was released back into culture medium starting within 24 h. A re-mobilization to this extent has not been previously observed.

The MTT assay was used to correlate the bioassociation behavior of Eu and U with the cell vitality. Speciation studies by spectroscopy and *in silico* methods highlighted various U and Eu species over the course of exposure. We were able to observe a new U species, which emerged simultaneously with the re-mobilization of U back into solution, which we assume to be a U(VI) phosphate species. Thus, the interaction of U(VI) and Eu(III) with released plant metabolites could be concluded.

KEYWORDS

Plant cells; Bioassociation; *Brassica napus*; Time-resolved laser-induced fluorescence spectroscopy; Radionuclides; Uranium; Europium; Speciation

SYNOPSIS

The re-mobilization of radionuclides and change in speciation following their interaction with plants may increase their threat to the environment.

TOC ART

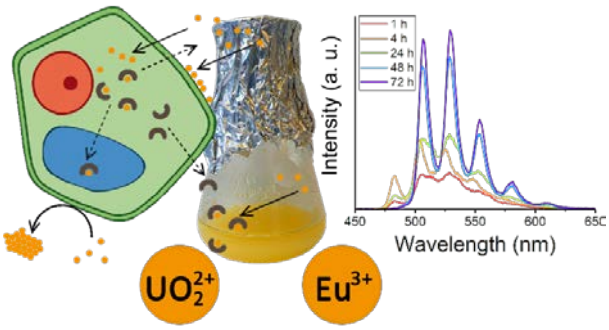


INTRODUCTION

The transfer behavior of radionuclides (RN) in the environment is a fundamental concern for both the remediation of radioactive contaminated sites, e.g., defunct sites of former uranium (U)

mining and milling operations, and the safety assessment of nuclear waste repositories. RN can enter the food chain via groundwater and soil and thus pose a health risk for both humans and wildlife.[1–3] As Laroche et al.[4] explained, the behavior of U in ecosystems is controlled by physicochemical and biological processes, which in turn are interrelated. For example, the biological release of organic substances, changes in pH, and soil carbonate and phosphate content can have a dramatic influence on speciation and therefore the mobility and bioavailability of U.[4–9]

Plants are key players in RN migration in soil and water bodies. There are a few studies pertaining to the interactions of RN with plants at the molecular level. These reports include investigations of plant cell cultures and whole plants, as well as modeling studies of RN transport within the plant.[3,4,6,10–23] However, most studies in this field focus on determining transfer factors. Consequently, there is currently insufficient information about the uptake processes taking place.[4]

The interaction processes[24] of RN with plant cells that have been reported include bioaccumulation of RN into the plant cell,[4,25–32] biosorption[33–35], as well as biocomplexation[36], biotransformation (here usually meant as bioreduction),[19] and bioprecipitation.[5,37] One aspect of these studies relates to complexation of U(VI) and europium (Eu(III)) with typical plant cell metabolites as ligands.[32,38–44] For the sake of simplicity, all processes that lead to an immobilization of RN can be encapsulated under the term *bioassociation*. This includes all cellular processes that contribute to less dissolved metal in the extracellular space and, consequently, less bioavailable metal for other organisms. With the exception of biocomplexation, this is the case for all processes described herein.[18,45,46]

Another aspect of these studies pertains to mechanistic investigations of U uptake. Sarthou et al.[47] reported that the cell wall, cell membranes, and external chelators represent a barrier for the

uptake of U into *Arabidopsis thaliana* plant cells. But this barrier can be surmounted, such that toxic metals are taken up to a limited extent into these cells, thereby causing interaction with intracellular biomolecules. For the same organism, Doustaly et al.[22] found evidence for metabolic pathways relating to iron uptake and homeostasis that are affected by U uptake, as well as an upregulation of genes involved in the activation of plant defense responses. Moreover, Serre et al.[10] also observed U-induced phosphate depletion and Fe redistribution in Arabidopsis root tissues. They proposed that U can increase Pi (inorganic phosphate) deficiency, again suggesting a connection to Fe homeostasis. In addition to this correlation, there are also indications for uptake of U in oat plant roots via pinocytosis[48] and in tobacco cells via Ca ion channels[36].

A deeper understanding of the migration behavior of RN cannot be achieved without knowledge of their respective species present in a biological system. Speciation is tremendously influential with respect to the bioavailability, and thus the toxicity, of RN to the organism.[2,4–6,15,29] Speciation is influenced by many factors, such as pH value, temperature, the presence of ligands for complexation (which includes metabolites), competitive ions, and the redox potential.[2,4–6,16] In this light, it is essential that phosphate concentration in nutrient media is kept to a minimum when investigating U speciation[6] and interaction, since complexes formed between U and phosphate are only barely soluble in water and, in fact, often precipitate out of solution, which can reduce the availability of U to the organism.[5,7,37,49] For speciation studies with U(VI)[17,18,20] and Eu(III) as analogues for trivalent actinides[26], time-resolved laser-induced fluorescence spectroscopy (TRLFS) represents a useful measurement tool. A combination of microscopy and TRLFS was applied to describe Eu(III) uptake and its partitioning behavior in the common oat (*Avena sativa*).[50]

Apart from U, determining the environmental behavior of trivalent actinides, like curium (Cm(III)) and americium (Am(III)), is no less important, especially since Am is known to play a

significant role in the radiotoxicity of radioactive waste in repository sites.[51,52] Fortunately, in order to model the interaction of Am(III) and Cm(III), Eu(III) can be used as a non-radioactive analogue for these actinides due to its ease of handling.[53]

Accordingly, this study was designed to investigate the interactions of U(VI) and Eu(III) with suspension cell cultures of *Brassica napus* (*B. napus*, rapeseed or canola) to contribute to a better understanding of the interaction processes of RN with plants at a molecular level. As a typical crop plant, rapeseed is a suitable model organism for study. In addition, *B. napus* is known to tolerate high levels of heavy metals and therefore is particularly suitable for process investigations.[29,49] The cell vitality, represented by the mitochondrial activity, as well as the amount of bioassociated (immobilized) metal were determined. In order to investigate the metal speciation, thermodynamic modeling and TRLFS studies were performed.

## MATERIALS AND METHODS

**Time- and concentration-dependent experiments.** For this study, callus-derived, dedifferentiated suspension cell cultures of *B. napus* were used, which were representative of germ-cell lines.[54] This was in order to ensure a uniform cell type, as opposed to a complex tissue, thus augmenting the ability to not only tightly control their growth conditions and stimulus exposure but also to minimize variations in other experimental factors that might arise from more complex model organisms. Moreover, as discussed by Zagoskina et al.[55], this approach also facilitates the ability to synthesize secondary metabolites. Due to the homogeneous, well-controlled properties, studies with plant suspension cell cultures, which can be used as a model system for whole plants, are appropriate for this purpose. The cell suspensions (40 mL, for cell cultivation see Supporting Information section and literature[17]) used for the experiments were

filtered through a nylon mesh (pore size 50 µm, Bückmann GmbH, Mönchengladbach, Germany) without suction and rinsed with 40 mL medium $R_{red}$. Medium $R_{red}$ represents a modified medium R with a reduced phosphate concentration of $6.25\times10^{-6}$ M (pH 5.8 ± 0.1), containing 0.5% of the original phosphate concentration (see Supporting Information, Table S1). The phosphate concentration was reduced in order to minimize the formation of Eu(III) and U(VI) phosphates. We do not suspect that P deficiency might cause too much stress as previous experiments have shown that *B. napus* plants show greater resistance to P starvation due to improved root system architecture traits.[56,57] Some of these particularities of the organism could also contribute to the ability of *B. napus* cells to cope with heavy metal stress under P deficiency. For the experiments, fresh cell-mass portions (1.5 g) were transferred into Erlenmeyer flasks. To study bioassociation processes as a function of the U(VI) / Eu(III) concentration, the U(VI) and Eu(III) concentrations in the cell cultivation medium were varied between 20 and 200 µM, and 30 and 200 µM, respectively. Accordingly, aliquots of a $1.11\times10^{-2}$ M or $9.45\times10^{-3}$ M $UO_2(NO_3)_2$ and $2.26\times10^{-2}$ M $EuCl_3$ stock solution were added to medium $R_{red}$, and the pH value of these solutions was adjusted to pH 5.8±0.1 (pH meter pH720, WTW inolab, Weilheim, Germany; with a Blue Line 16 pH electrode, SI Analytics, Mainz, Germany). Subsequently, 10 mL of these solutions were added to the cells. Note that control samples were prepared without U(VI) and Eu(III) in the same way. Incubation was carried out on a horizontal shaker (model SM-30; Edmund Bühler GmbH, Bodelshausen, Germany) under slight agitation at room temperature. The exposure time was fixed at 24 h. For the time-dependent experiments, cell culture media with fixed concentrations of U(VI) (20 and 200 µM) and Eu(III) (30 and 200 µM) were prepared, after which the cells were exposed to these media for 1, 4, 24, 48, and 72 h. After exposure, the cells were separated from the medium. The supernatants were then centrifuged (11,000 rpm, room temperature; centrifuge 5804R,

Eppendorf, Hamburg, Germany). Inductively coupled plasma mass spectrometry (ICP-MS; models NexION 350x, Perkin Elmer, Rodgau, Germany and iCapRQ, Thermo Fisher Scientific, Dreieich, Germany) was used to determine the concentrations of U(VI) and Eu(III) in the medium before and after cell exposure. The amount of bioassociated metal (as a percentage of the initial amount of metal in the medium) was calculated (see Supporting Information for further information). After separation, the cells were washed with 10 mL medium $R_{red}$, and cell vitality was measured (see below).

For the time-dependent experiments, a series of three independent experiments was performed for the control and for each heavy metal concentration at each time step. Over the different exposure times, the pH of the supernatants varied between 4.5 and 6.7. To determine the concentration-dependent data, two independent experiments with three samples for the control and each heavy metal concentration in parallel were evaluated. The pH values of the nutrient solutions varied between pH 4.4 and 6.3 after 24 h of exposure.

**Vitality measurements.** An MTT assay[58,59] was performed to measure cell vitality. This test allows the determination of reductase activity of cytosolic and mitochondrial dehydrogenases, and is considered a proxy for general cellular metabolism.[60] For this study, a yellow water-soluble 3-(4,5-dimethylthiazol-2-yl)-2,5-diphenyltetrazolium bromide (MTT, Duchefa, Haarlem, The Netherlands) substrate was added to the cells, which was enzymatically reduced to the blue, water-insoluble formazan product. Cell vitality was determined using the MTT test, as described by Sachs et al.[17], immediately after separating the supernatants from the cells (see Supporting Information for further details). For each individual sample of the time-dependent experiments, the MTT assay was performed twice; in contrast, one MTT assay was conducted for each sample of the concentration-dependent experiments, still yielding ample data for statistical relevance.

Accordingly, the mean values and standard errors of the mean (SEM) for the cell vitalities were calculated based on six measurements: for the concentration-dependent experiments, for each concentration studied, there were two experiments, each with three flasks, for which one MTT test per flask was performed; for the time-dependent experiments, for each concentration and exposure time, there were three experiments, each with one flask, for which two MTT tests per flask were performed. The cell vitality of the U(VI) and Eu(III) exposed cells was expressed as a percentage based on the determined absorbance value of the mean of the control samples.

**Statistical analysis.** A two-tailed Student's t-test was performed for the statistical evaluation of cell vitality data using Microsoft Excel 2016 and the implemented "Analysis ToolPak" function. In particular, the p-value was used to determine whether cell vitality data deviated significantly from the mean value for the control cell vitalities. One asterisk (*) represents statistical significance ($p < 0.05$), while two asterisks (**) indicate a very significant deviation ($p < 0.01$).

**TRLFS approach.** TRLFS measurements were performed to determine the U(VI) and Eu(III) speciation in the biological system. Information about the investigated samples and their preparation can be found in the Supporting Information. Measuring the U(VI) samples was performed at low temperatures (-120 °C) to reduce the background noise generated by the autofluorescence of organic components.[61] Plastic cuvettes (Roth, Rotilabo disposable UV cuvettes, XK26.1) were used for measurements. The samples were frozen in liquid nitrogen and stored at -80 °C until measurement. More detailed information regarding the U(VI) TRLFS measurements were described in detail before[36] and can be found in the Supporting Information section.

All TRLFS data were analyzed using OriginPro 2015G and Origin 2017 (OriginLab Corporation, Northampton, MA), utilizing parallel factor analysis (PARAFAC) with MATLAB 6.0 software (The Mathworks Corporation, Natick, MA) as described in the literature.[62]

The TRLFS studies with the Eu(III) samples were performed as previously described.[63,64] More information regarding the measurements can be found in the Supporting Information section. The supernatant samples were placed in 1 cm quartz glass cuvettes (Hellma Analytics, Mühlheim, Germany) and measured. The luminescence spectra were evaluated by factor analysis (ITFA: iterative target factor analysis) as described in the literature.[62,65] The spectrum of the $Eu^{3+}$ aquo ion as a reference was included in the ITFA calculations. Spectra were normalized to the area of the $^5D_0 \rightarrow {}^7F_1$ transition (magnetic dipole), since this transition is not influenced by the chemical environment of the Eu(III). The relative peak intensity ($I$) ratio ($R_{E/M}$) was calculated according to equation 2:

$$R_{E/M} = I(\,{}^5D_0 \rightarrow {}^7F_2)/I(\,{}^5D_0 \rightarrow {}^7F_1) \qquad (2)$$

The number of coordinated water molecules was determined based on the equation of Kimura et al.[66], which is presented for Eu(III) in equation 3:

$$N_{H_2O} = 1.07\, k_{exp} - 0.62 \qquad (3)$$

($N_{H_2O}$ – coordination number of water molecules, $k_{exp}$ – reciprocal luminescence emission lifetime (ms)).

## RESULTS AND DISCUSSION

**Concentration-dependent experiments.** To investigate the relationship between the U(VI) and Eu(III) concentrations and the degree of heavy metal bioassociation, we conducted concentration-dependent experiments. The exposure time was fixed at 24 h, while the heavy metal concentrations

were varied from 20 to 200 µM (U(VI)) and from 30 to 200 µM (Eu(III)). The absolute amount of bioassociated heavy metal (see Supporting Information, Figure S1) increased linearly with increasing metal concentration in the medium. Moreover, there was no saturation effect with respect to the amount of metal associated with the cells, since independent of the initial concentration, a maximum of about 83% (U(VI)) or 75% (Eu(III)) was bioassociated (representing a relative consideration of bioassociation in percent; see Supporting Information, Figure S2). This process can be described by linear regression results: the $R^2$ values were 0.990 for U(VI) and 0.995 for Eu(III). It should also be noted that cell vitality levels for the samples with heavy metal concentrations of 100 µM and less remained at the level of the control samples (about 100%; see Supporting Information, Figure S2). With increasing U(VI) concentration, however, a significant increase in cell vitality was observed (for 200 µM U(VI)). Conversely, for Eu(III), a slight decrease in cell vitality occurred with increasing Eu(III) concentration, which was significant for 200 µM Eu(III). The changes in cell vitalities are discussed in more detail for the time-dependent studies of bioassociation.

**Time-dependent experiments.** We used different concentrations of U(VI) (20, 200 µM) and Eu(III) (30, 200 µM) to study the time-dependent bioassociation with *B. napus* cells. Figure 1 illustrates the level of bioassociated metal and cell vitality as a function of exposure time for both 20 and 200 µM U(VI), and 30 and 200 µM Eu(III).

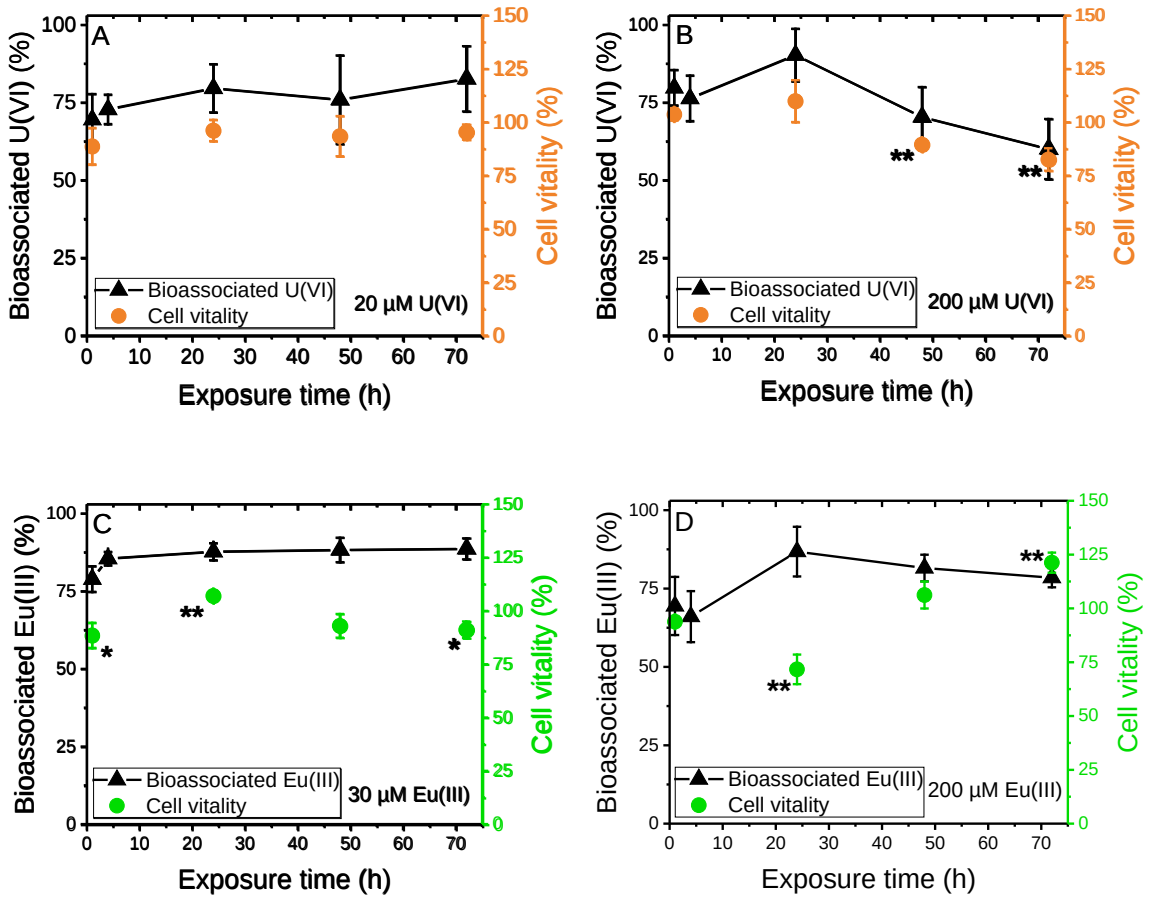


**Figure 1.** Amount of bioassociated heavy metal and cell vitality results for *B. napus* cells exposed to A) 20 µM U(VI), B) 200 µM U(VI), C) 30 µM Eu(III), and D) 200 µM Eu(III). Data represent mean values ± SEM of three independent experiments. Compared to the unexposed control cells, significant differences in cell vitality were confirmed using Student's t-test. One asterisk (*) denotes statistical significance ($p < 0.05$), and two asterisks (**) indicates a very significant event ($p < 0.01$).

As indicated in Figure 1A, C, and D, a similar bioassociation process was observed for 20 µM U(VI), as well as for 30 and 200 µM Eu(III). Specifically, after a rapid initial increase in the amount of bioassociated heavy metal, an equilibrium state was reached after about 24 h exposure time, at which point, up to 85% of the total heavy metal amount was bioassociated by the plant

cells. Similar to what we observed in our concentration-dependent studies, complete bioassociation did not occur in our time-dependent investigations, which we attribute to the fact that cells were actively involved in maintaining this state of equilibrium. It is conceivable that the initial rapid increase was mainly due to biosorption, which tends to occur very quickly, since this process does not require the active uptake of the heavy metal into the cell, as indicated by a study involving green algae *Chlorella vulgaris*.[35] This statement is supported by Sarthou et al.[47] who showed that cell walls play an important role in binding U and thus contribute significantly to its immobilization. Rajabi et al.[36] were able to show that after only 1 h of exposure, U(VI) was taken up by *Nicotiana tabacum* BY-2 cells. Moll et al.[67] were able to show by cell fractionation that for *B. napus* callus cells, most of the U and Eu is bound to the heavy cell components (cell wall fraction) and only a small fraction was found in the cytoplasm. Electron microscopy images of oat plant roots[48] prove that already after short incubation times, U appears abundantly in all areas of the cell, but especially massively at the cell walls. These images illustrate the chemically plausible assumption that sorption, as an energetically passive process, is a major contributor to immobilization, but that uptake of the metals into the cell nevertheless occurs together with other processes, such as complexation and precipitation. This equilibrium-related behavior can also be attributed to additionally active interaction processes between the cell and the heavy metal, like uptake of the heavy metals via different pathways such as ion channels[36] or endocytosis[48]. According to the current state of knowledge, however, it is not yet possible to reliably differentiate between the processes involved. The interpretation of our time-dependent bioassociation data reveals similarities to other observations of biosorption in the literature that have performed kinetic modeling and report models that fit the mechanisms of sorption by *B. napus*. For example, a comparable trend was observed by El Hayek et al. in their hydroponic experiments for U uptake

in *Brassica juncea* roots at concentrations of 0.1 to 2.9 µM U(VI).[68] As described in the literature[68–70], the bioassociation process detailed here for *B. napus* was modelled as a sorption process using different fit functions (fit models with first, second, and pseudo-first order kinetics). As in the case of El Hayek et al., the best agreement corresponds to a second-order kinetics model.[68] Nevertheless, this fit should only be considered to be an approximation, since more than just sorption processes occur in a biological system. Experimental evidence by Laurette et al.[49] showed that U is not only taken up into plant cells but may also be sequestered as precipitates in the vacuoles. Also, Rajabi et al.[36] investigated Ca ion channels as potential uptake pathways of U in *N. tabacum* BY-2 cells over short exposure times. For *B. napus* suspension cells, we demonstrated the uptake of U into the cells by transmission electron microscopy (TEM) combined with energy-dispersive X-ray spectroscopy (EDXS) analysis as well, showing precipitation of uranium and phosphorus in the form of needles, and sorption of uranium to intracellular phospholipid membranes (see Supporting Information Figure S3). The prominent presence of uranium inside the cell argues for active uptake and possible sequestering mechanisms at play in these cells. In the case of 20 µM U(VI), cell vitality remained at the level of the control samples at about 100%. For 30 µM Eu(III), however, cell vitality slightly increased at 24 h of exposure but then decreased beginning at about 72 h. A significant decrease in cell vitality was observed for 200 µM Eu(III) up to 24 h, which can likely be attributed to a lower metabolic activity of the plant cells due to the increased Eu(III) concentration and the associated heavy metal stress. Here, it looks like the cells downregulate their metabolic activity around 24 h of exposure due to the heavy metal load. Cell death seems to be an unlikely explanation for this event, since the time-dependent experiments (Figure 1D) only show an intermittent decrease in vitality followed by a significant increase. It seems to be rather a decrease of total metabolic activity as a consequence of severe

heavy metal exposure, where the cells are in a state of shock. It can only be speculated why this vitality decrease does not occur for 200 µM U(VI). After 24 h of exposure, there is a larger increase in bioassociation of Eu(III) compared to U(VI). It could therefore be that the shock state of the Eu(III) exposed cells is caused by this larger increase in metal loading. Similarly, the increased cell vitality for the higher exposure times (72 h) can be explained as a metabolic stress response of the cells. The increased cell vitality can be explained here by the fact that exposure to heavy metals can induce a stress response and thereby drive energy-requiring processes in the cell. The additionally required energy is produced by an increase in the necessary enzymes, among which is the mitochondrial dehydrogenase, resulting in an increased metabolic activity.

For 200 µM U(VI), a different bioassociation behavior was observed. The time-dependent data for 200 µM U(VI) showed a rapid increase in bioassociation that was found to be similar to that at the lower U(VI) concentration of 20 µM, which might be associated with sorption as described earlier. Subsequently, a reproducible decrease in the amount of bioassociated U(VI) was observed, indicating a release reaction taking place through which U(VI) was again mobilized. It is conceivable that this release represents a defense reaction of the cells. In particular, in addition to the active release of U(VI)-complexing metabolites, a release of complexing cell components as a result of cell lysis due to cell death from the heavy metal load could also be a contributing factor. The following TRLFS results may help shed more light on this.

The complexation with cell components or metabolites could thus be accompanied by the increased mobility of U(VI), which results in an increased concentration of U(VI) in the supernatants. In the literature, however, such behavior was also observed for the bioassociation of U(VI) with tobacco suspension cell cultures[36], although in a less pronounced form. Bader et al. described a multistage bioassociation for halophilic archaea *Halobacterium noricense* within an

exposure period of 24 h.[45,46] As far as we know, this is the first time that a multistage bioassociation process has been observed for U with plant (*B. napus*) cells with a release of bound U to this intensity. Through the formation of metabolites by the cell, U can be complexed and released back into the nutrient medium. Indeed, previous studies have detailed the release of protective metabolites, such as phenols and flavonoids (which can complex heavy metals), as a typical defense mechanism for plants exposed to such contaminants to reduce their bioavailability.[38,71–73] When considering the time-dependent data for 200 µM U(VI), however, we observed distinct variations in the initiation of U release by the plant cells (see Supporting Information, Figure S4) for the individual experiments, which we cannot yet attribute to any specific factor or combination of factors.

The toxicity of U(VI) in these experiments can mainly be attributed to its chemotoxicity as a heavy metal. In contrast, a radiotoxic effect can be excluded due to the very long half-life of natural U. Cell vitality data for 200 µM U(VI) remained approximately constant at the level of the control samples for 1 to 24 h and was found to decrease for longer exposure times from 48 up to 72 h (Figure 1B). Reduced cell vitality of approximately 80% (72 h) compared to the control (100%) can be attributed to a decrease in metabolic activity, probably due to the beginning of cell death caused by U exposure.

**U(VI)-TRLFS.** TRLFS was used to investigate the supernatants and cells of the time-dependent experiments with *B. napus* cells exposed to 200 µM U(VI). Since comparable results were obtained for all experiments, the data presented and described here refer specifically to experimental results with cells of the 2$^{nd}$ passage, but are representative of the full measurement series. The measurements were carried out dynamically so that time-resolved spectra were

obtained. Figure 2 shows the spectra of the supernatants at the different exposure times, as well as provides the spectrum of the initial medium (200 µM U(VI)) after a delay of 0.1 µs.

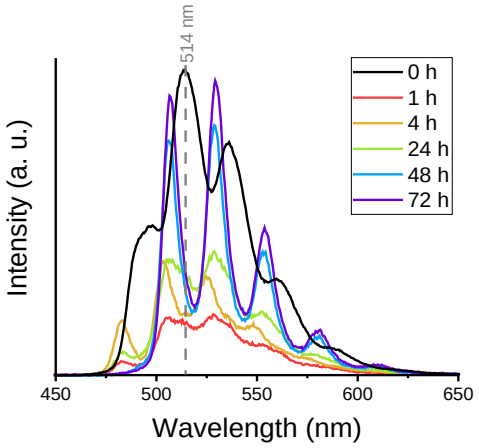


**Figure 2.** U(VI) luminescence spectra after a delay of 0.1 µs of the supernatants from cells exposed to 200 µM U(VI) for different exposure times and the initial medium containing 200 µM U(VI).

Recorded changes during exposure time verified that U(VI) speciation in the supernatants differed from results obtained for the initial medium. The spectra of the dynamic measurements were evaluated using the factor analysis code PARAFAC to identify the species that contributed to the sum spectra; this algorithm was also implemented to determine their distribution. The obtained single-component spectra of these species, the spectrum of the free $UO_2^{2+}$ ion for comparison (main peak 509 nm[62]), as well as the species distribution based on the luminescence intensity over the exposure time are shown in Figure 3.

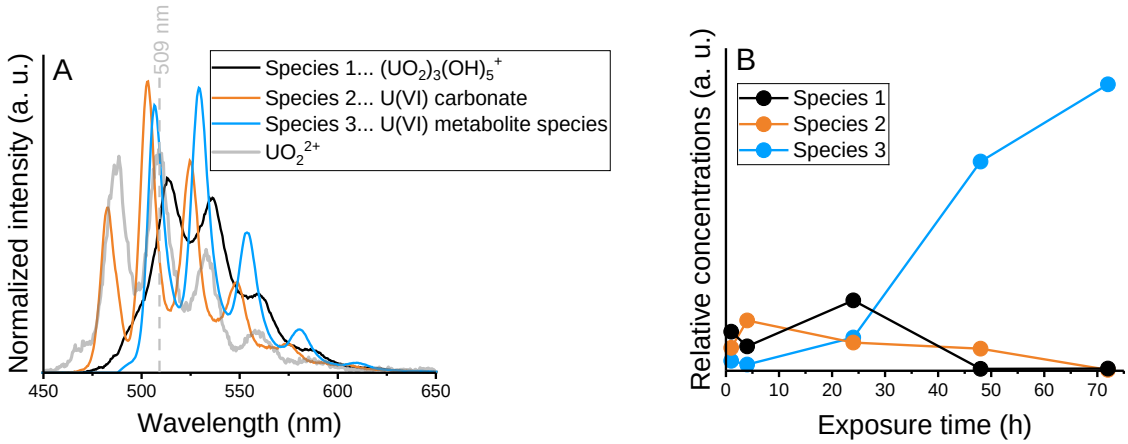


**Figure 3.** PARAFAC results: A) extracted single-component spectra of the species present in the supernatants of *B. napus* cells exposed to 200 µM U(VI) for different exposure times and the reference spectrum of $UO_2^{2+}$ for comparison, and B) calculated species distribution based on luminescence intensities (amount of bioassociated metal considered).

All measurements were performed under cryogenic conditions. Because the precise quenching mechanisms that take place at these low temperatures are not yet fully understood, luminescence lifetime data will not be discussed in detail. Nonetheless, this data can be used as starting point for comparing the detected species in the different experiments, since results should be similar for the same species. By looking at luminescence lifetimes (not shown) and comparing the band positions (see Supporting Information, Table S4), three species could be determined for all experiments performed. Time-dependent differences were noted, which were expected based on identified bioassociation processes (see Supporting Information, Figure S4).

Prior to the exposure of cells, the speciation of U(VI) in the initial culture medium was modeled, and $(UO_2)_3(OH)_5^+$ was found to be the dominant species under our conditions. The results of this modeling can be found in the Supporting Information (Figure S5 and Table S2). Using these calculations, insight into U(VI) speciation in the aqueous phase can be obtained. However, these

calculations represent only an estimation of actual conditions, since no additional input into the solutions (chemical components, surfaces, etc.) associated with the cellular material, which definitely control the behavior of the metals in the system, are considered.

At the onset, species 1 was identified, which refers to the initial species $(UO_2)_3(OH)_5^+$ in the medium. Thus, it could be proven spectroscopically that for 200 µM U(VI), the dominant species was the $(UO_2)_3(OH)_5^+$ complex, as predicted by the thermodynamic calculations (see Supporting Information, Figure S5 and Table S2) and in the literature.[17]

Species 2, which occurred intermediately and evidenced a slight blue shift compared to the $UO_2^{2+}$ ion, was probably a U(VI) carbonate[74] species. The formation of a U(VI) carbonate species can be explained by cellular respiration, during which $CO_2$ is released by the cells.[45] This implies that the occurrence of species 2 is expected in supernatants solely after contact with living plant cells. The notion of a U(VI) species resulting from cell respiration is corroborated by the study with *N. tabacum* suspension cell cultures.[36] Their results highlight that a spectrum resembling that of species 2 largely occurred as long as the cells were alive, and this was independent of metabolic changes resulting from a sufficiency or deficiency of iron. In contrast, other U(VI) species in their study showed a dependence on metabolic changes affected by iron. Moreover, exposing dead, autoclaved cells to fresh medium $R_{red}$ containing 200 µM U(VI) did not show the occurrence of species 2 by TRLFS (data not shown). A comparison between the spectrum of species 2 and a reference spectrum of $UO_2(CO_3)$ showed strong resemblance (Figure S8 in Supporting Information). According to modeling calculations (see Supporting Information Figure S5 and Table S2), the proportion of the $UO_2(CO_3)$ complex under the initial medium conditions is expected to be less than 1%. However, cell respiration may lead to a steady increase of the carbonate content in the nutrient medium, so that an occurrence of this species can be expected. It

can therefore be assumed that species 2 is the $UO_2(CO_3)$ complex or a chemically very similar but modified carbonate species, possibly with other, additional ligands.

With increasing exposure time, we noted the appearance of species 3, which showed a significant redshift of its band positions compared to the free $UO_2^{2+}$ ion. Importantly, species 3 appeared in all experiments precisely at the point at which U(VI) began to be released from the cells, following the trend shown in Figure 1B. Interestingly, the emergence of this species in TRLFS studies was also evident upon two other conditions: one, an exposure of U(VI) to an aqueous (pH 5) lysate of autoclaved *B. napus* cells; and two, an exposure of U(VI) to a cell-free supernatant of a 72 h old phosphate-deficient $R_{red}$ culture that was previously unexposed to U(VI) (data not shown). Taken together, these observations suggest that this species is the result of a metabolite or biomolecule that is likely intracellular and released in response to a stressor (heavy metal or P deficiency) and/or is the result of cell death and lysis, which then complexes with surface-bound U(VI) and eventually leads to its re-mobilization.

For the identification of species 3, we obtained TRLFS spectra of selected potential metabolites complexed with U(VI) (Figure S9) to identify matching spectra to species 3. Ideally, different groups of metabolites should be considered. For example, phenolic compounds and flavonoids are mentioned in the literature as typical secondary metabolites that are formed by the plant under heavy metal stress[38]. Inorganic compounds and small organic molecules, such as the polyhydroxy acids and dicarboxylic acids, have been considered as well[24,38]; these include fumaric acid, m/p-coumaric acid, ferulic acid, GSSG (glutathione, oxidized form), phytic acid, acetate, citrate, lactate, and various carbonate and phosphate species. Unfortunately, species 3 has not yet been identified using these approaches (see Supporting Information for exemplary reference spectra in

Figure S9 and a list of all references investigated with TRLFS) and the use of reference spectra from the literature. Due to the large number of possible metabolites and their derivatives, it is spectroscopically very difficult to identify a single species. However, a redshift as strong as that observed for species 3 has been observed for inorganic U(VI) phosphate species, and the band positions of species 3 are similar to those of inorganic phosphates ($UO_2PO_4^-$, $UO_2HPO_4$, $UO_2H_2PO_4^+$, $UO_2(H_2PO_4)_2$)[75,76] or complexes of U(VI) with organic phosphates such as glycerol-1-phosphate[77] (measurements at room temperature), albeit, slightly more red-shifted. We therefore assume that the ligand involved in the formation of species 3 is an (organic or inorganic) phosphate. Due to the strong affinity of U to phosphate, it would be expected that in case of a release of (organic) phosphates, U bound to them would enter the surrounding nutrient medium, which may explain the significant increase in U concentration and the associated decrease in bioassociation, respectively (Figure 1).

Based on the vitality data, it is reasonable to assume that cell death and lysis contribute partially to the release of U(VI) (Figure 1B). However, there are also points arguing against it. Firstly, our concentration-dependent experiments show, there is no saturation of bioassociation with metal concentrations up to 200 µM and hence an ample presence of binding ligands. Since cell-surface sorption, being a kinetically rapid process, is expected to be the primary form of bioassociation, the observed re-mobilization of U cannot only be explained by a release of intracellular U. There would also have to be a detachment and dissolution of U complexes from cell surfaces. Secondly, intracellular U present will very unlikely be freely available and rather immobilized or strongly complexed (e.g., precipitation in vacuoles). Therefore, upon lysis, this complexed U will have to be mobilized by stronger-binding ligands to account for the increase in soluble U in the medium. Thirdly, U species that are released from the cell by lysis and have similar binding capabilities as

U species in the initial medium, will rapidly be adsorbed to cell debris and dead biomass. If, however, a specific metabolite was released to complex U, there will be a lower likelihood of immobilization on cell debris. Fourthly, *B. napus* cell cultures showed a more pronounced release of U compared to *N. tabacum* cells, despite the decrease in the vitality not being as strong as the decrease in viability of *N. tabacum*.[36] Although in this case, no direct correlation with cell viability is possible, a vitality of 80% for *B. napus* leaves for an assumption that there were sufficiently more living cells, compared to an only 50% viable tobacco cell population. Nevertheless, the hypothesis of lysis-mediated U release is supported by the point that a release of phosphates is to be expected only in exceptional situations of the cells due to the physiological importance of this nutrient. As this discussion shows, a final statement on this topic is not possible according to the current state of knowledge. It can be assumed that cell lysis plays a role in the release of U(VI), however, the strength of the decrease in U(VI) bioassociation cannot be explained by this alone. In addition to cell lysis, we suppose cellular stress response to be responsible for the release of the complexing metabolites.

Cryogenic TRLFS measurements of *B. napus* cell biomass (see Supporting Information, Figure S10) confirmed that the occurrence of one species remained unchanged over the entire exposure time. Moreover, the band positions of this species were observed to be very similar to those of a U(VI) root and shoot species published by Günther et al.[18] This spectrum can be attributed to the binding of U(VI) to the cell membrane; specifically, functional groups on the surface of the cells (biomembranes) are available as binding partners for U(VI). It is assumed that U(VI) binds to organic phosphate groups of phospholipids, for example. This hypothesis is supported by studies of Panak et al.[78] with bacterial strains (*Bacillus* isolates). Here, very strong similarities of the *B. napus* U(VI) cell spectrum to the spectra of $UO_2(HPO_4)_{(aq)}$ recorded at room

temperature and also to those of some of the U isolate species are found. Panak et al.[78] used different techniques, such as room temperature TRLFS and extended X-ray absorption fine structure (EXAFS) spectroscopic studies. Their results led to the conclusion that the binding of U(VI) occurs predominantly via outer cell components with phosphate residues, such as polysaccharides or phospholipids. Although these studies were performed with bacterial strains, there is a basic similarity with other biomembranes, since plant cell walls and membranes also contain phosphate groups for the binding of U(VI). More detailed TRLFS studies of U(VI) cell species for *B. napus* cells can be found in the literature.[20,67]

**Eu(III)-TRLFS.** TRLFS was also utilized to study the supernatants of the time-dependent experiments of *B. napus* cells exposed to 200 µM Eu(III). The luminescence spectra of the initial medium $R_{red}$ with an Eu(III) concentration of 200 µM and of the supernatants after cell exposure to 200 µM Eu(III) are shown in Figure 4.

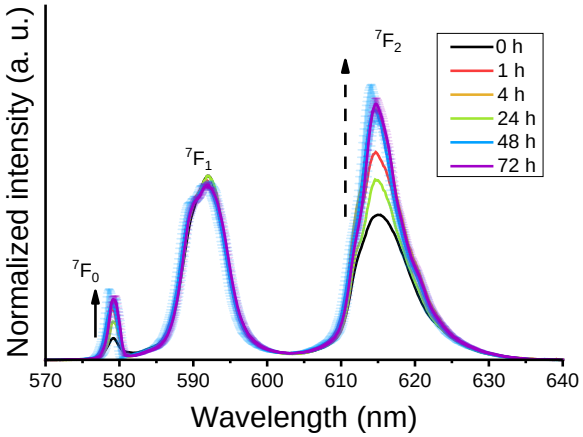


**Figure 4.** Luminescence spectra of the initial medium $R_{red}$ (200 µM Eu(III)) and the supernatants from cells exposed to 200 µM Eu(III) for different exposure times after a delay of 1 µs. Results of two independent experiments are shown.

Modeling calculations were performed for the medium prior to cell contact, indicating a dominant role of the free $Eu^{3+}$ ion, with Eu(III) sulfate and nitrate also appearing, albeit to a lesser

extent (see Supporting Information, Figures S6 and S7 and Table S3). These spectra indicate that starting from the initial medium with 200 µM Eu(III), a speciation change occurred in the supernatants after cell contact; this phenomenon was also confirmed by the relative peak intensity ratio ($R_{E/M}$) (see Supporting Information, Table S5). The $^5D_0 \rightarrow {}^7F_0$ transition is already visible in the medium. This transition is spin forbidden and cannot be observed for highly symmetric complexes with an inversion center such as $(Eu(H_2O)_9)^{3+}$ ($D_{3h}$). However, it can occur for Eu(III) complexes of low symmetry (without an inversion center), which was also found to be the case for the medium $R_{red}$ with Eu(III) and for the supernatants. The intensity of this transition increased noticeably with exposure time. In examining the hypersensitive transition $^5D_0 \rightarrow {}^7F_2$, first a significant increase in intensity between 0 and 1 h of incubation time was detected followed by a constant intensity, which is strongly dependent on the symmetry of the Eu(III) and thus on the type of bound ligands. This observed correlation between the fast increase in intensity and increasing exposure time indicates a newly formed species, which appeared to have a significantly different symmetry than the species present in the initial medium. To further analyze these data, the Eu(III) TRLFS spectra of the supernatants after cell contact and with a delay of 1 µs were evaluated using ITFA.[65] Figure 5 shows the calculated single-component spectra and the species distribution with the initial $R_{red}$ medium with Eu(III).

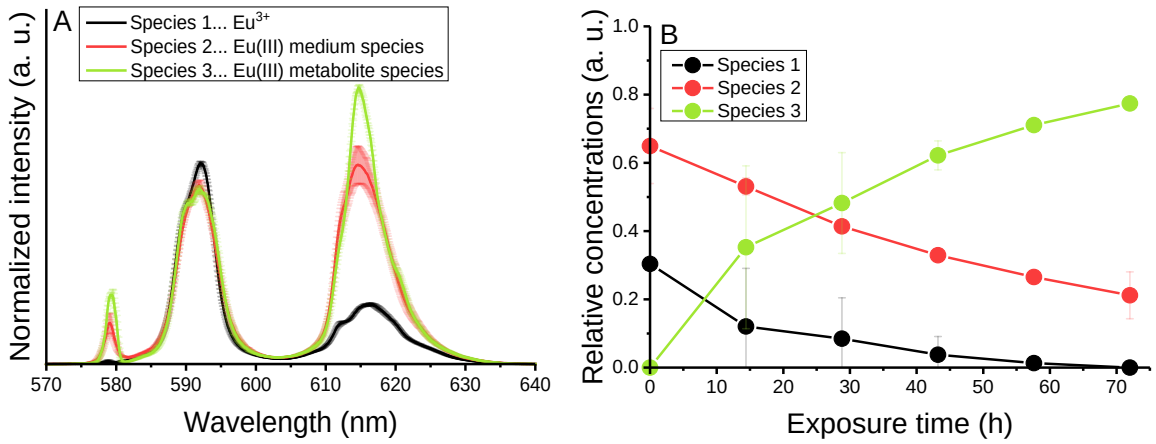

**Figure 5.** ITFA results: A) extracted single-component spectra of Eu(III) species in the supernatants from *B. napus* cells exposed to 200 µM Eu(III) for different exposure times and B) the calculated species distribution (amount of bioassociated metal not considered). Data represent mean values ± standard deviation.

Species 1 can be attributed to the $Eu^{3+}$ aquo ion, which was present in the medium together with Eu(III) complexes with components of the medium (species 2). Both species were found to be dominant in the initial medium (t = 0 h). However, once species 3 appeared in the supernatants after 1 h of exposure time, it then suppressed species 1 and 2 with increasing exposure times. Therefore, we propose that species 3 could be an Eu(III) species with metabolite ligands. For Eu(III), we have estimated the relative intensities of species 1, 2, and 3 from the measured luminescence intensities and by using the relative species distribution presented in Figure 5B. The relative luminescence intensity (FI) of species 1, $Eu^{3+}$, was set to 1. The relative FIs of species 2 and 3 were calculated to be 1.84 and 0.27, respectively. On the basis of experimental data, the possible influence of carbonate resulting from cell respiration cannot be excluded, as ternary complexes could be formed. However, an accurate allocation of the type of involved functionalities has yet to be performed. It should also be noted that a review of the luminescence lifetime data confirmed that bi-exponential decays occurred both in the medium $R_{red}$ with Eu(III) and in the supernatants, indicating that two Eu(III) coordination environments were dominant. Moreover, we observed an extension of both lifetimes in all supernatants compared to the medium $R_{red}$. Table S6 provides luminescence lifetime results for the Eu(III) species in both the initial medium ($[Eu(III)]_0$: 200 µM) and for the supernatants after contact with *B. napus* cells with 200 µM Eu(III). The detected lifetimes of the bi-exponential decay represent the sum parameter for all present species. On the basis of our findings, however, we were unable to assign the average lifetimes to the three

species. In the first approximation, the contribution of the $Eu^{3+}$ aquo ion was visible in the short lifetime. Data for the prolonged lifetime of the long-lived component confirmed the increasing influence of metabolites on Eu(III) complexation, as evidenced by the fact that the number of coordinated water molecules in this species decreased to three (see Supporting Information, Table S6). It is remarkable that the short-lived species 2 displayed a shorter lifetime (80 or 105 µs) than the $Eu^{3+}$ ion (111 µs).[79] Indeed, a decrease in the OH-induced quenching of the water molecules bound in the first coordination sphere was observed in Eu(III) complexing reactions where water molecules are replaced by ligand molecules. This would result in prolonged luminescence lifetimes. The observed decrease in the short lifetime may be an indication of additional ligand-specific quenching processes (e.g. complex ligand mixture in the medium $R_{red}$ and the supernatants), which have already been described in the literature for biological systems.[79] The spectra of cells exposed to Eu(III) are not discussed here. For a detailed study of Eu(III) cell species, we refer to the TRLFS measurements of *B. napus* cells by Moll et al.[67,80]

A significant body of scholarly reports indicates that the interaction of RN with plant cells or other organisms results in the bioassociation of the RN, possibly leading to the immobilization of the respective RN. The results from this investigation, however, clearly indicate that this behavior cannot be applied to all plant cells. In our study, a pronounced multistage bioassociation behavior with U(VI) was observed for the first time for *B. napus* plant cells, resulting in the release of the RN by the plant cells after initial bioassociation. Such behavior was also observed for tobacco suspension cell cultures[36], although in a less pronounced form. Our spectroscopic investigations confirmed that speciation of U(VI) and Eu(III) in the supernatants was influenced by the plant cells. In this work, suitable spectroscopic methods have been used to detect biocomplexation in such an extent directly in the biological system of plant cells as a sub-process at the cellular level.

Accordingly, this knowledge should be incorporated in any environmental risk assessment involving radionuclides and the modeling of their transfer behaviors up to the food chain. Work in this field should be considered an important step forward in understanding the processes taking place on a molecular level. Such knowledge is highly relevant for the remediation of former uranium mining and milling facilities, as well as applies to the deep disposal of solid radioactive waste. An important finding from this study is that cell components or metabolites released by plant cells can be involved in mobilization processes of RN such as biocomplexation. Nonetheless, future work in this field should address the challenge of identifying released plant cell metabolites and to investigate their complex formation behavior with RN.

## ASSOCIATED CONTENT

**Supporting Information**. Supporting Information for this work is available free of charge on the ACS publication website at DOI: XXX. Additional details on the composition of medium $R_{red}$, the calculation of the bioassociated amount of heavy metals, the thermodynamic modeling of the U(VI) and Eu(III) speciation in medium $R_{red}$, and analysis of TRLFS data (PDF) can also be accessed there.

## AUTHOR INFORMATION


### Corresponding Author

*E-mail: s.sachs@hzdr.de (S.S.).



### Funding Sources

The research is part of the joint project "TRANS-LARA" (Transport and transfer behavior of long-lived radionuclides along the pathway groundwater - soil - surface - plant under consideration of long-term climatic changes), which is funded by the Federal Ministry of Education and Research under contract number 02NUK051B.

**Notes**

The authors declare no competing financial interest.

## ACKNOWLEDGMENT

The authors thank J. Seibt and S. Heller for their valuable help with the performance of the experiments, Dr. M. Bader, A. Wollenberg, and H. Neubert for cryo TRLFS measurements of U(VI) references and S. Beutner and S. Bachmann for ICP-MS measurements. We also thank Laurie S. Good for proofreading the manuscript. We thank T. Kurth from the Center of Regenerative Therapies Dresden (CRTD) for the preparation of thin sections of *B. napus* cells. Furthermore, the use of the HZDR Ion Beam Center TEM facilities and the funding of TEM Talos by the German Federal Ministry of Education of Research (BMBF; grant No. 03SF0451) in the framework of HEMCP are acknowledged.

## REFERENCES

(1) Bernhard, G.; Geipel, G.; Brendler, V.; Nitsche, H. Uranium Speciation in Waters of Different Uranium Mining Areas. *J. Alloys Compd.* **1998**, *271–273*, 201–205. https://doi.org/10.1016/S0925-8388(98)00054-1.

(2) Sheppard, S. C.; Evenden, W. G. Critical Complilation of Plant/Soil Concentration Ratios for Uranium, Thorium and Lead. *J. Environ. Radioact.* **1988**, *8* (3), 255–285.

(3) Gupta, D. K.; Chatterjee, S.; Mitra, A.; Voronina, A.; Walther, C. Uranium and Plants: Elemental Translocation and Phytoremediation Approaches. In *Uranium in Plants and the Environment*; Gupta, D. K., Walther, C., Eds.; Springer International Publishing: Cham, 2020; pp 149–161. https://doi.org/10.1007/978-3-030-14961-1_7.

(4) Laroche, L.; Henner, P.; Camilleri, V.; Morello, M.; Garnier-Laplace, J. Root Uptake of Uranium by a Higher Plant Model (*Phaseolus Vulgaris*) - Bioavailability from Soil Solution. *Radioprotection* **2005**, *40* (S1), 33–39. https://doi.org/10.1051/radiopro.

(5) Laurette, J.; Larue, C.; Llorens, I.; Jaillard, D.; Jouneau, P.-H.; Bourguignon, J.; Carrière, M. Speciation of Uranium in Plants upon Root Accumulation and Root-to-Shoot Translocation: A XAS and TEM Study. *Environ. Exp. Bot.* **2012**, *77*, 87–95. https://doi.org/10.1016/j.envexpbot.2011.11.005.

(6) Ebbs, S. D.; Brady, D. J.; Kochian, L. V. Role of Uranium Speciation in the Uptake and Translocation of Uranium by Plants. *J. Exp. Bot.* **1998**, *49* (324), 1183–1190. https://doi.org/10.1093/jxb/49.324.1183.

(7) Henner, P.; Brédoire, F.; Tailliez, A.; Coppin, F.; Pierrisnard, S.; Camilleri, V.; Keller, C. Influence of Root Exudation of White Lupine (*Lupinus Albus L.*) on Uranium Phytoavailability in a Naturally Uranium-Rich Soil. *J. Environ. Radioact.* **2018**, *190–191*, 39–50. https://doi.org/https://doi.org/10.1016/j.jenvrad.2018.04.022.

(8) Soudek, P.; Petrová, Š.; Buzek, M.; Lhotský, O.; Vaněk, T. Uranium Uptake in *Nicotiana Sp.* under Hydroponic Conditions. *J. Geochemical Explor.* **2014**, *142*, 130–137. https://doi.org/10.1016/j.gexplo.2013.10.001.

(9) Saenen, E.; Horemans, N.; Vanhoudt, N.; Vandenhove, H.; Biermans, G.; Van Hees, M.; Wannijn, J.; Vangronsveld, J.; Cuypers, A. Effects of pH on Uranium Uptake and Oxidative Stress Responses Induced in *Arabidopsis Thaliana*. *Environ. Toxicol. Chem.* **2013**, *32* (9), 2125–2133. https://doi.org/10.1002/etc.2290.

(10) Serre, N. B. C.; Alban, C.; Bourguignon, J.; Ravanel, S. Uncovering the Physiological and Cellular Effects of Uranium on the Root System of *Arabidopsis Thaliana*. *Environ. Exp. Bot.* **2019**, *157* (October 2018), 121–130. https://doi.org/10.1016/j.envexpbot.2018.10.004.

(11) Gupta, D. K.; Vuković, A.; Semenishchev, V. S.; Inouhe, M.; Walther, C. Uranium Accumulation and Its Phytotoxicity Symptoms in *Pisum Sativum L*. *Environ. Sci. Pollut. Res.* **2020**, *27* (3), 3513–3522. https://doi.org/10.1007/s11356-019-07068-9.

(12) Chen, X.; Wu, G.; Ma, Q.; Lai, J.; Luo, X.; Ji, X. Cytotoxic and Genotoxic Evaluation and the Toxicological Mechanism of Uranium in *Vicia Faba* Root. *Environ. Exp. Bot.* **2020**, *179*, 104227. https://doi.org/https://doi.org/10.1016/j.envexpbot.2020.104227.

(13) Lai, J.; Liu, Z.; Luo, X. A Metabolomic, Transcriptomic Profiling, and Mineral Nutrient Metabolism Study of the Phytotoxicity Mechanism of Uranium. *J. Hazard. Mater.* **2020**, *386*, 121437. https://doi.org/https://doi.org/10.1016/j.jhazmat.2019.121437.

(14) Zhang, Y.; Lai, J.-L.; Ji, X.-H.; Luo, X.-G. Unraveling Response Mechanism of Photosynthetic Metabolism and Respiratory Metabolism to Uranium-Exposure in *Vicia Faba*. *J. Hazard. Mater.* **2020**, *398*, 122997. https://doi.org/https://doi.org/10.1016/j.jhazmat.2020.122997.

(15) Hu, N.; Zhang, H.; Ding, D.; Tan, Y.; Li, G. Influence of Uranium Speciation on Plant Uptake. In *Uranium in Plants and the Environment*; Gupta, D. K., Walther, C., Eds.;

Springer International Publishing: Cham, 2020; pp 181–191. https://doi.org/10.1007/978-3-030-14961-1_9.

(16) Iurian, A.-R.; Phaneuf, M. O.; Mabit, L. Mobility and Bioavailability of Radionuclides in Soils. In *Radionuclides in the Environment: Influence of chemical speciation and plant uptake on radionuclide migration*; Walther, C., Gupta, D. K., Eds.; Springer International Publishing: Cham, 2015; pp 37–59. https://doi.org/10.1007/978-3-319-22171-7_2.

(17) Sachs, S.; Geipel, G.; Bok, F.; Oertel, J.; Fahmy, K. Calorimetrically Determined U(VI) Toxicity in *Brassica Napus* Correlates with Oxidoreductase Activity and U(VI) Speciation. *Environ. Sci. Technol.* **2017**, *51* (18), 10843–10849. https://doi.org/10.1021/acs.est.7b02564.

(18) Günther, A.; Bernhard, G.; Geipel, G.; Reich, T.; Roßberg, A.; Nitsche, H. Uranium Speciation in Plants. *Radiochim. Acta* **2003**, *91* (6), 319–328. https://doi.org/10.1524/ract.91.6.319.20022.

(19) Viehweger, K.; Geipel, G.; Bernhard, G. Impact of Uranium (U) on the Cellular Glutathione Pool and Resultant Consequences for the Redox Status of U. *Biometals* **2011**, *24*, 1197–1204. https://doi.org/10.1007/s10534-011-9478-6.

(20) Geipel, G.; Viehweger, K. Speciation of Uranium in Compartments of Living Cells. *BioMetals* **2015**, *28* (3), 529–539. https://doi.org/10.1007/s10534-015-9836-x.

(21) Boghi, A.; Roose, T.; Kirk, G. J. D. A Model of Uranium Uptake by Plant Roots Allowing for Root-Induced Changes in the Soil. *Environ. Sci. Technol.* **2018**, *52* (6), 3536–3545. https://doi.org/10.1021/acs.est.7b06136.

(22) Doustaly, F.; Combes, F.; Fiévet, J. B.; Berthet, S.; Hugouvieux, V.; Bastien, O.; Aranjuelo, I.; Leonhardt, N.; Rivasseau, C.; Carrière, M.; Vavasseur, A.; Renou, J. P.;

Vandenbrouck, Y.; Bourguignon, J. Uranium Perturbs Signaling and Iron Uptake Response in *Arabidopsis Thaliana* Roots. *Metallomics* **2014**, *6* (4), 809–821. https://doi.org/10.1039/c4mt00005f.

(23) Berthet, S.; Villiers, F.; Alban, C.; Serre, N. B. C.; Martin-Laffon, J.; Figuet, S.; Boisson, A. M.; Bligny, R.; Kuntz, M.; Finazzi, G.; Ravanel, S.; Bourguignon, J. *Arabidopsis Thaliana* Plants Challenged with Uranium Reveal New Insights into Iron and Phosphate Homeostasis. *New Phytol.* **2018**, *217* (2), 657–670. https://doi.org/10.1111/nph.14865.

(24) Francis, A. J. Biotransformation of Uranium and Other Actinides in Radioactive Wastes. *J. Alloys Compd.* **1998**, *271–273*, 78–84. https://doi.org/10.1016/S0925-8388(98)00028-0.

(25) Gao, Y.; Zeng, F.; Yi, A.; Ping, S.; Jing, L. Research of the Entry of Rare Earth Elements $Eu^{3+}$ and $La^{3+}$ into Plant Cell. *Biol. Trace Elem. Res.* **2003**, *91* (3), 253–265.

(26) Zha, Z.; Wang, D.; Hong, W.; Liu, L.; Zhou, S.; Feng, X.; Qin, B.; Wang, J.; Yang, Y.; Du, L.; Zhang, D.; Fang, Z.; Xia, C. Influence of Europium Speciation on Its Accumulation in *Brassica Napus* and Over-Expressing BnTR1 Lines. *J. Radioanal. Nucl. Chem.* **2014**, *301* (1), 257–262. https://doi.org/10.1007/s10967-014-3120-3.

(27) Singh, S.; Malhotra, R.; Bajwa, B. S. Uranium Uptake Studies in Some Plants. *Radiat. Meas.* **2005**, *40* (2–6), 666–669. https://doi.org/10.1016/j.radmeas.2005.01.013.

(28) Vanhoudt, N.; Vandenhove, H.; Horemans, N.; Bello, D. M.; van Hees, M.; Wannijn, J.; Carleer, R.; Vangronsveld, J.; Cuypers, A. Uranium Induced Effects on Development and Mineral Nutrition of *Arabidopsis Thaliana*. *J. Plant Nutr.* **2011**, *34* (13), 1940–1956. https://doi.org/10.1080/01904167.2011.610482.

(29) Chang, P.; Kim, K. W.; Yoshida, S.; Kim, S. Y. Uranium Accumulation of Crop Plants Enhanced by Citric Acid. *Environ. Geochem. Health* **2005**, *27* (5–6), 529–538.

https://doi.org/10.1007/s10653-005-8013-5.

(30) Tomé, F. V.; Rodríguez, P. B.; Lozano, J. C. The Ability of *Helianthus Annuus L*. and *Brassica Juncea* to Uptake and Translocate Natural Uranium and 226Ra under Different Milieu Conditions. *Chemosphere* **2009**, *74*, 293–300. https://doi.org/10.1016/j.chemosphere.2008.09.002.

(31) Kaur, A.; Singh, S.; Virk, H. S. A Study of Uranium Uptake in Plants. *Nucl. Tracks Radiat. Meas.* **1988**, *15* (1–4), 795–798.

(32) Qi, F.; Zha, Z.; Du, L.; Feng, X.; Wang, D.; Zhang, D.; Fang, Z.; Ma, L.; Jin, Y.; Xia, C. Impact of Mixed Low-Molecular-Weight Organic Acids on Uranium Accumulation and Distribution in a Variant of Mustard (*Brassica Juncea* Var. *Tumida*). *J. Radioanal. Nucl. Chem.* **2014**, *302* (1), 149–159. https://doi.org/10.1007/s10967-014-3279-7.

(33) Sheppard, M. I.; Vandergraaf, T. T.; Thibault, D. H.; Keith Reid, J. A. Technetium and Uranium: Sorption by and Plant Uptake from Peat and Sand. *Health Phys.* **1983**, *44* (6), 635–643. https://doi.org/10.1097/00004032-198306000-00004.

(34) Khani, M. H.; Keshtkar, A. R.; Ghannadi, M.; Pahlavanzadeh, H. Equilibrium, Kinetic and Thermodynamic Study of the Biosorption of Uranium onto *Cystoseria Indica* Algae. *J. Hazard. Mater.* **2008**, *150* (3), 612–618. https://doi.org/10.1016/j.jhazmat.2007.05.010.

(35) Vogel, M.; Günther, A.; Rossberg, A.; Li, B.; Bernhard, G.; Raff, J. Biosorption of U(VI) by the Green Algae *Chlorella Vulgaris* in Dependence of PH Value and Cell Activity. *Sci. Total Environ.* **2010**, *49* (324), 384–395. https://doi.org/10.1016/j.scitotenv.2010.10.011.

(36) Rajabi, F.; Jessat, J.; Garimella, J. N.; Bok, F.; Steudtner, R.; Stumpf, T.; Sachs, S. Uranium (VI) Toxicity in Tobacco BY-2 Cell Suspension Culture – A Physiological Study. *Ecotoxicol. Environ. Saf.* **2021**, *211*, 111883.

https://doi.org/10.1016/j.ecoenv.2020.111883.

(37) Misson, J.; Henner, P.; Morello, M.; Floriani, M.; Wu, T.; Guerquin-Kern, J.-L.; Février, L. Use of Phosphate to Avoid Uranium Toxicity in *Arabidopsis Thaliana* Leads to Alterations of Morphological and Physiological Responses Regulated by Phosphate Availability. *Environ. Exp. Bot.* **2009**, *67*, 353–362. https://doi.org/10.1016/j.envexpbot.2009.09.001.

(38) Viehweger, K. How Plants Cope with Heavy Metals. *Bot. Stud.* **2014**, *55* (1), 1–12. https://doi.org/10.1186/1999-3110-55-35.

(39) Pasilis, S. P.; Pemberton, J. E. Speciation and Coordination Chemistry of Uranyl(VI)-Citrate Complexes in Aqueous Solution. *Inorg. Chem.* **2003**, *42* (21), 6793–6800. https://doi.org/10.1021/ic0341800.

(40) Günther, A.; Geipel, G.; Bernhard, G. Complex Formation of U(VI) with the Amino Acid *L*-Threonine and the Corresponding Phosphate Ester O-Phospho-*L*-Threonine. *Radiochim. Acta* **2006**, *94* (12), 845–851.

(41) Rawat, N.; Bhattacharyya, A.; Tomar, B. S.; Ghanty, T. K.; Manchanda, V. K. Thermodynamics of U(VI) and Eu(III) Complexation by Unsaturated Carboxylates. *Thermochim. Acta* **2011**, *518* (1–2), 111–118.

(42) Günther, A.; Steudtner, R.; Schmeide, K.; Bernhard, G. Luminescence Properties of Uranium(VI) Citrate and Uranium(VI) Oxalate Species and Their Application in the Determination of Complex Formation Constants. *Radiochim. Acta* **2011**, *99* (9), 535–542. https://doi.org/10.1524/ract.2011.1847.

(43) Brachmann, A.; Geipel, G.; Bernhard, G.; Nitsche, H. Study of Uranyl (VI) Malonate Complexation by Time Resolved Laser-Induced Fluorescence Spectroscopy (TRLFS).

*Radiochim. Acta* **2002**, *90*, 147–153.

(44) Frost, L.; Geipel, G.; Viehweger, K.; Bernhard, G. Interaction of Uranium(VI) towards Glutathione – an Example to Study Different Functional Groups in One Molecule. *Proc. Radiochem. A Suppl. to Radiochim. Acta* **2011**, *1* (1), 357–362. https://doi.org/10.1524/rcpr.2011.0063.

(45) Bader, M.; Rossberg, A.; Steudtner, R.; Drobot, B.; Großmann, K.; Schmidt, M.; Musat, N.; Stumpf, T.; Ikeda-Ohno, A.; Cherkouk, A. Impact of Haloarchaea on Speciation of Uranium - A Multispectroscopic Approach. *Environ. Sci. Technol.* **2018**, *52* (21), 12895–12904. https://doi.org/10.1021/acs.est.8b02667.

(46) Bader, M.; Müller, K.; Foerstendorf, H.; Drobot, B.; Schmidt, M.; Musat, N.; Swanson, J. S.; Reed, D. T.; Stumpf, T.; Cherkouk, A. Multistage Bioassociation of Uranium onto an Extremely Halophilic Archaeon Revealed by a Unique Combination of Spectroscopic and Microscopic Techniques. *J. Hazard. Mater.* **2017**, *327*, 225–232. https://doi.org/10.1016/j.jhazmat.2016.12.053.

(47) Sarthou, M. C. M.; Revel, B. H.; Villiers, F.; Alban, C.; Bonnot, T.; Gigarel, O.; Boisson, A. M.; Ravanel, S.; Bourguignon, J. Development of a Metalloproteomic Approach to Analyse the Response of Arabidopsis Cells to Uranium Stress. *Metallomics* **2020**, *12* (8), 1302–1313. https://doi.org/10.1039/d0mt00092b.

(48) Wheeler, H.; Hanchey, P. Pinocytosis and Membrane Dilation in Uranyl-Treated Plant Roots. *Science (80-. ).* **1971**, *171* (3966), 68–71. https://doi.org/10.1126/science.171.3966.68.

(49) Laurette, J.; Larue, C.; Mariet, C.; Brisset, F.; Khodja, H.; Bourguignon, J.; Carrière, M. Influence of Uranium Speciation on Its Accumulation and Translocation in Three Plant

Species: Oilseed Rape, Sunflower and Wheat. *Environ. Exp. Bot.* **2012**, *77*, 96–107. https://doi.org/10.1016/j.envexpbot.2011.11.007.

(50) Fellows, R. J.; Wang, Z.; Ainsworth, C. C. Europium Uptake and Partitioning in Oat (*Avena Sativa*) Roots as Studied by Laser-Induced Fluorescence Spectroscopy and Confocal Microscopy Profiling Technique. *Environ. Sci. Technol.* **2003**, *37* (22), 5247–5253. https://doi.org/10.1021/es0343609.

(51) Salvatores, M. *Physics and Safety of Transmutation Systems - A Status Report*; Nuclear Energy Agency: Paris, 2006.

(52) Westlén, D. Reducing Radiotoxicity in the Long Run. *Prog. Nucl. Energy* **2007**, *49* (8), 597–605.

(53) Ansoborlo, E.; Prat, O.; Moisy, P.; Den Auwer, C.; Guilbaud, P.; Carriere, M.; Gouget, B.; Duffield, J.; Doizi, D.; Vercouter, T.; Moulin, C.; Moulin, V. Actinide Speciation in Relation to Biological Processes. *Biochimie* **2006**, *88* (11), 1605–1618. https://doi.org/10.1016/j.biochi.2006.06.011.

(54) Fehér, A. Callus, Dedifferentiation, Totipotency, Somatic Embryogenesis: What These Terms Mean in the Era of Molecular Plant Biology? *Front. Plant Sci.* **2019**, *10*, 536. https://doi.org/10.3389/fpls.2019.00536.

(55) Zagoskina, N. V.; Goncharuk, E. A.; Alyavina, A. K. Effect of Cadmium on the Phenolic Compounds Formation in the Callus Cultures Derived from Various Organs of the Tea Plant. *Russ. J. Plant Physiol.* **2007**, *54* (2), 237–243.

(56) Wang, X.; Chen, Y.; Thomas, C. L.; Ding, G.; Xu, P.; Shi, D.; Grandke, F.; Jin, K.; Cai, H.; Xu, F.; Yi, B.; Broadley, M. R.; Shi, L. Genetic Variants Associated with the Root System Architecture of Oilseed Rape (*Brassica Napus L.*) under Contrasting Phosphate

Supply. *DNA Res.* **2017**, *24* (4), 407–417. https://doi.org/10.1093/dnares/dsx013.

(57) Shi, L.; Shi, T.; Broadley, M. R.; White, P. J.; Long, Y.; Meng, J.; Xu, F.; Hammond, J. P. High-Throughput Root Phenotyping Screens Identify Genetic Loci Associated with Root Architectural Traits in *Brassica Napus* under Contrasting Phosphate Availabilities. *Ann. Bot.* **2013**, *112* (2), 381–389. https://doi.org/10.1093/aob/mcs245.

(58) Lindl, T.; Gstraunthaler, G. *Zell- Und Gewebekultur*, 6th ed.; Spektrum Akademischer Verlag: Heidelberg, 2008.

(59) Mosmann, T. Rapid Colorimetric Assay for Cellular Growth and Survival: Application to Proliferation and Cytotoxicity Assays. *J. Immunol. Methods* **1983**, *65*, 55–63.

(60) Kupcsik, L. Estimation of Cell Number Based on Metabolic Activity: The MTT Reduction Assay. In *Mammalian Cell Viability. Methods in Molceluar Biology (Methods and Protocols)*; Stoddart, M. J., Ed.; Humana Press, 2011; pp 13–19. https://doi.org/https://doi.org/10.1007/978-1-61779-108-6_3.

(61) Steudtner, R.; Arnold, T.; Geipel, G.; Bernhard, G. Fluorescence Spectroscopic Study on Complexation of Uranium(VI) by Glucose: A Comparison of Room and Low Temperature Measurements. *J. Radioanal. Nucl. Chem.* **2010**, *284* (2), 421–429. https://doi.org/10.1007/s10967-010-0489-5.

(62) Drobot, B.; Steudtner, R.; Raff, J.; Geipel, G.; Brendler, V.; Tsushima, S. Combining Luminescence Spectroscopy, Parallel Factor Analysis and Quantum Chemistry to Reveal Metal Speciation – a Case Study of Uranyl(VI) Hydrolysis. *Chem. Sci.* **2015**, *6*, 964–972. https://doi.org/10.1039/C4SC02022G.

(63) Moll, H.; Lütke, L.; Bachvarova, V.; Cherkouk, A.; Selenska-Pobell, S.; Bernhard, G. Interactions of the Mont Terri Opalinus Clay Isolate *Sporomusa* Sp. MT-2.99 with

Curium(III) and Europium(III). *Geomicrobiol. J.* **2014**, *31* (8), 682–696. https://doi.org/10.1080/01490451.2014.889975.

(64) Moll, H.; Johnsson, A.; Schäfer, M.; Pedersen, K.; Budzikiewicz, H.; Bernhard, G. Curium(III) Complexation with Pyoverdins Secreted by a Groundwater Strain of *Pseudomonas Fluorescens*. *BioMetals* **2008**, *21* (2), 219–228. https://doi.org/10.1007/s10534-007-9111-x.

(65) Roßberg, A.; Reich, T.; Bernhard, G. Complexation of Uranium(VI) with Protocatechuic Acid-Application of Iterative Transformation Factor Analysis to EXAFS Spectroscopy. *Anal. Bioanal. Chem.* **2003**, *376* (5), 631–638. https://doi.org/10.1007/s00216-003-1963-5.

(66) Kimura, T.; Choppin, G. R.; Kato, Y.; Yoshida, Z. Determination of the Hydration Number of Cm(III) in Various Aqueous Solutions. *Radiochim. Acta* **1996**, *72* (2), 61–64. https://doi.org/10.1524/ract.1996.72.2.61.

(67) Moll, H.; Sachs, S.; Geipel, G. Plant Cell (*Brassica Napus*) Response to Europium(III) and Uranium(VI) Exposure. *Environ. Sci. Pollut. Res.* **2020**, *27* (25), 32048–32061. https://doi.org/10.1007/s11356-020-09525-2.

(68) El Hayek, E.; Torres, C.; Rodriguez-Freire, L.; Blake, J. M.; De Vore, C. L.; Brearley, A. J.; Spilde, M. N.; Cabaniss, S.; Ali, A. M. S.; Cerrato, J. M. Effect of Calcium on the Bioavailability of Dissolved Uranium(VI) in Plant Roots under Circumneutral pH. *Environ. Sci. Technol.* **2018**, *52* (22), 13089–13098. https://doi.org/10.1021/acs.est.8b02724.

(69) Keskinkan, O.; Goksu, M. Z. L.; Basibuyuk, M.; Forster, C. F. Heavy Metal Adsorption Properties of a Submerged Aquatic Plant (*Ceratophyllum Demersum*). *Bioresour. Technol.*

**2004**, *92* (2), 197–200. https://doi.org/10.1016/j.biortech.2003.07.011.

(70) Hossain, A.; Bhattacharyya, S. R.; Aditya, G. Biosorption of Cadmium by Waste Shell Dust of Fresh Water Mussel *Lamellidens Marginalis*: Implications for Metal Bioremediation. *ACS Sustain. Chem. Eng.* **2015**, *3* (1), 1–8. https://doi.org/10.1021/sc500635e.

(71) Emamverdian, A.; Ding, Y.; Mokhberdoran, F.; Xie, Y. Heavy Metal Stress and Some Mechanisms of Plant Defense Response. *Sci. World J.* **2015**, *2015*, 1–19. https://doi.org/10.1155/2015/756120.

(72) Weiler, E.; Nover, L. *Allgemeine Und Molekulare Botanik*, 1st ed.; Georg Thieme Verlag: Stuttgart, 2008.

(73) Sytar, O.; Kumar, A.; Latowski, D.; Kuczynska, P.; Strzałka, K.; Prasad, M. N. V. Heavy Metal-Induced Oxidative Damage, Defense Reactions, and Detoxification Mechanisms in Plants. *Acta Physiologiae Plantarum*. 2013, pp 985–999. https://doi.org/10.1007/s11738-012-1169-6.

(74) Wang, Z.; Zachara, J. M.; Yantasee, W.; Gassman, P. L.; Liu, C.; Joly, A. G. Cryogenic Laser Induced Fluorescence Characterization of U(VI) in Hanford Vadose Zone Pore Waters. *Environ. Sci. Technol.* **2004**, *38* (21), 5591–5597. https://doi.org/10.1021/es049512u.

(75) Bonhoure, I.; Meca, S.; Marti, V.; De Pablo, J.; Cortina, J. L. A New Time-Resolved Laser-Induced Fluorescence Spectrometry (TRLFS) Data Acquisition Procedure Applied to the Uranyl-Phosphate System. *Radiochim. Acta* **2007**, *95* (3), 165–172. https://doi.org/10.1524/ract.2007.95.3.165.

(76) Kirishima, A.; Kimura, T.; Tochiyama, O.; Yoshida, Z. Speciation Study on Complex

Formation of Uranium(VI) with Phosphate and Fluoride at High Temperatures and Pressures by Time-Resolved Laser-Induced Fluorescence Spectroscopy. *Radiochim. Acta* **2004**, *92* (12), 889–896. https://doi.org/10.1524/ract.92.12.889.55111.

(77) Koban, A.; Bernhard, G. Complexation of Uranium(VI) with Glycerol 1-Phosphate. *Polyhedron* **2004**, *23* (10), 1793–1797. https://doi.org/10.1016/j.poly.2004.04.022.

(78) Panak, P. J.; Raff, J.; Selenska-Pobell, S.; Geipel, G.; Bernhard, G.; Nitsche, H. Complex Formation of U(VI) with Bacillus-Isolates from a Uranium Mining Waste Pile. *Radiochim. Acta* **2000**, *88* (2), 71–76. https://doi.org/10.1524/ract.2000.88.2.071.

(79) Kuke, S.; Marmodée, B.; Eidner, S.; Schilde, U.; Kumke, M. U. Intramolecular Deactivation Processes in Complexes of Salicylic Acid or Glycolic Acid with Eu(III). *Spectrochim. Acta - Part A Mol. Biomol. Spectrosc.* **2010**, *75* (4), 1333–1340. https://doi.org/10.1016/j.saa.2009.12.080.

(80) Moll, H.; Schmidt, M.; Sachs, S. Curium(III) and Europium(III) as Luminescence Probes for Plant Cell (*Brassica Napus*) Interactions with Potentially Toxic Metals. *J. Hazard. Mater.* **2021**, *412*, 125251. https://doi.org/https://doi.org/10.1016/j.jhazmat.2021.125251.